IEEE Robotics and Automation Letters (RAL) paper presented at the
2020 IEEE International Conference on Robotics and Automation (ICRA)
31 May - 31 August, 2020. Paris, France

Discovering Interpretable Dynamics by Sparsity Promotion on Energy and the Lagrangian

Hoang K. Chu and Mitsuhiro Hayashibe

***Abstract*—Data-driven modeling frameworks that adopt sparse regression techniques, such as sparse identification of nonlinear dynamics (SINDy) and its modifications, are developed to resolve difficulties in extracting underlying dynamics from experimental data. In contrast to neural-network-based methods, these methods are designed to obtain white-box analytical models. In this work, we incorporate the concept of SINDy and knowledge in the field of classical mechanics to identify interpretable and sparse expressions of total energy and the Lagrangian that shelters the hidden dynamics. Moreover, our method (hereafter referred as Lagrangian-SINDy) is developed to use knowledge of simple systems that form the system being analyzed to ensure the likelihood of correct results and to improve the learning pace. Lagrangian-SINDy is highly accurate in discovering interpretable dynamics via energy-related physical quantities. Its performance is validated with three popular multi-DOF nonlinear dynamical systems, namely the spherical pendulum, double pendulum and cart-pendulum system. Comparisons with other SINDy-based methods are made and Lagrangian-SINDy is found to provide the most compact analytical models.**

***Index Terms*—Dynamics, Calibration and Identification Dynamics, Model Learning for Control**

I. Introduction and Related Works

MANKIND'S understanding of laws underlying physical phenomena has resulted in achievements in various fields and especially in physics, from Newtonian mechanics to the theory of relativity. A knowledge of natural laws provides not only an accurate relation between cause and effect but also the possibility of prediction in unseen situations.

Machine learning [1] and big data [2]—two modern data-driven techniques of finding meaningful relations in an abundance of data—have inspired scientists to create artificial intelligence that is comparable to the intelligence of humans in several tasks; for example, classification and labeling. However, there is a huge gap between a machine and a human in terms of adaptability, flexibility and learning pace.

Playing with a cup-and-ball toy is an example of numerous tasks for which humans show a profound understanding of physical phenomena and a wonderful ability of predicting transitions. The toy comprises a rod with a cup attached to one end and a pendulum comprising a mass and a string, and the task is to swing the mass such that it falls into the cup. The majority of people can swing the mass higher than the cup in first trials and successfully complete the task after a short time. Apparently, this progress is not simply fortuitous; that is, people understand the physics of the pendulum to a certain extent and they use that knowledge to understand a more complex system. The main motivation of the present work is the design of machines that understand physical laws autonomously and use known phenomena to effectively accelerate learning.

Many efforts have been made to tackle the task of autonomously learning physical laws. Machine learning models (e.g., neural networks), which are frequently black boxes [3], are used to find relations between input and output, yet do not provide much insight into how the relations are formed. Interpretable models, in contrast to black boxes, are more desirable thanks to their ability to provide causal connections, especially in new situations where data availability is limited.

Remarkable progress was made by [4] in terms of showing that it is possible to distill natural laws from experimental data. That work employed symbolic regression to find a model that is sufficiently accurate while maintaining reasonable model complexity. Furthermore, it was hinted that the learning rate improves if laws of a simpler system are used to bootstrap the learning process.

Recent works [5], [6] made notable progress in terms of making neural network models more transparent. A shallow neural network made of explicit linear and nonlinear neurons was shown to be capable of modeling complex functions in an interpretable manner.

Sparse identification of nonlinear dynamics [7] (SINDy) emerged as an effective method of finding underlying dynamics. This method models dynamics by forming a linear combination of nonlinear basis functions and adopts a sparse regression technique to accomplish the same goal as that achieved in [4]. Many modifications of SINDy have been proposed; e.g., SINDy-PDE [8], SINDy-c [9], implicit-SINDy [10], and abrupt-SINDy [11].

Koopman reduced-order nonlinear identification and control (KRONIC) [12]—which is based on SINDy—is able to identify conservation laws [13]. Invariants are fundamental principles for most physical systems [4], [13]. They not only indicate constraints on motions but also provide clues for estimating and predicting the evolution of a system. One of the most important quantities is energy, as it allows the reformulation of classical mechanics [14].

In the present work, we propose a method based on SINDy and KRONIC that more efficiently realizes the discovery of

This work was supported by the JSPS Grant-in-Aid for Scientific Research (B), no. 18H01399. *(Corresponding author: Hoang K. Chu)*

The authors are with Neuro-Robotics Lab, Department of Robotics, Graduate School of Engineering, Tohoku University, 980-8579, Sendai, Japan. Email: khanhhoang@dc.tohoku.ac.jp; hayashibe@tohoku.ac.jp

interpretable dynamics via the Hamiltonian and Lagrangian (summarized in Fig. 1). The main contributions of this work are:

1) development of a scheme based on KRONIC that finds energy in a system having multiple degrees of freedom (DOFs) using prior knowledge of energy in simpler systems,
2) development of a method of finding the Lagrangian from the total energy and experimental data, and
3) demonstration of the effectiveness of Lagrangian-SINDy in popular physical systems.

Section II introduces how we use basic ideas of related works and our development. Section III presents results of experiments conducted on several physical systems. Section IV gives closing remarks.

II. Method

A. Learning energy in a multi-DOF system using prior knowledge of energy in simple systems

Following the concept of SINDy that a function can be presented as a linear combination of nonlinear terms, the total energy of a system (i.e., the sum of kinetic energy and potential energy) is constructed as the sum of various terms such that each term is a function of state. Using a vector $\mathbf{x}(t)$ to represent the state at time t, the total energy of the system is expressed as

$$\text{TotalEnergy} = \sum_{k=1}^{p} \theta_k(\mathbf{x}(t))\xi_k, \tag{1}$$

where $\boldsymbol{\Theta}(\mathbf{x}) = [\theta_1(\mathbf{x}(t))\,\theta_2(\mathbf{x}(t))\cdots\theta_p(\mathbf{x}(t))]$ is the library of candidate functions and $\boldsymbol{\xi} = [\xi_1\,\xi_2\cdots\xi_p]$ is the vector of coefficients. To solve (1), data are collected at times $t_1, t_2, \cdots, t_m$. A matrix containing the time history of the state is formed as $\mathbf{X} = [\mathbf{x}(t_1)\,\mathbf{x}(t_2)...\mathbf{x}(t_m)]$, and its derivative $\dot{\mathbf{X}} = [\dot{\mathbf{x}}(t_1)\,\dot{\mathbf{x}}(t_2)\cdots\dot{\mathbf{x}}(t_m)]$ can be either measured directly or approximated numerically [7]. Once a data matrix $\boldsymbol{\Theta}(\mathbf{X}) = [\boldsymbol{\theta}_1(\mathbf{X}^T)\,\boldsymbol{\theta}_2(\mathbf{X}^T)...\boldsymbol{\theta}_p(\mathbf{X}^T)]$ is generated, (1) is further developed (denoting the vector of energy at times that data were collected as $\mathbf{E}$) as

$$\mathbf{E} = \boldsymbol{\Theta}(\mathbf{X})\boldsymbol{\xi}. \tag{2}$$

In the next step, by following the process of KRONIC, we construct $\boldsymbol{\Gamma}(\mathbf{X}, \dot{\mathbf{X}})$—the time-derivative matrix of $\boldsymbol{\Theta}(\mathbf{X})$. Each column of $\boldsymbol{\Gamma}(\mathbf{X}, \dot{\mathbf{X}})$ is calculated using the chain rule and represents the time derivative of a basis function that $\boldsymbol{\Theta}(\mathbf{X})$ contains. The calculation is summarized as

$$\boldsymbol{\Gamma}(\mathbf{X}, \dot{\mathbf{X}}) = [\nabla\boldsymbol{\theta}_1(\mathbf{X}^T)\cdot\dot{\mathbf{X}}\,\nabla\boldsymbol{\theta}_2(\mathbf{X}^T)\cdot\dot{\mathbf{X}}\cdots\nabla\boldsymbol{\theta}_p(\mathbf{X}^T)\cdot\dot{\mathbf{X}}]. \tag{3}$$

It is logical to exclude all constant functions in $\boldsymbol{\Theta}(\mathbf{X})$ as they eventually give several columns of zeros in $\boldsymbol{\Gamma}(\mathbf{X}, \dot{\mathbf{X}})$, which are meaningless. A vector denoting the time derivative of the energy $\frac{d\mathbf{E}}{dt}$ is formulated by $\boldsymbol{\Gamma}(\mathbf{X}, \dot{\mathbf{X}})$ and $\boldsymbol{\xi}$:

$$\boldsymbol{\Gamma}(\mathbf{X}, \dot{\mathbf{X}})\boldsymbol{\xi} = \frac{d\mathbf{E}}{dt}. \tag{4}$$

In a mechanical system, the rate of energy being supplied or withdrawn is a crucial factor that is usually measurable or controllable. Some control signals (e.g., a force or torque) directly affect how the total energy of a system varies over time, while others require further calculation to unveil their relations to energy. In this work, we assume that data on how the total energy changes $\frac{d\mathbf{E}}{dt}$ are available.

If no energy is supplied or withdrawn (i.e., the right-hand side of (4) is a vector of zeros), then $\boldsymbol{\xi}$ is in the null space of $\boldsymbol{\Gamma}(\mathbf{X}, \dot{\mathbf{X}})$ and it is thus possible to obtain by adopting singular value decomposition [15]. If the total energy changes, regression techniques (e.g., least-square regression) can be used to solve for $\boldsymbol{\xi}$. Other sparse regression techniques (e.g., Ridge [16], Lasso [17]) can be used for a sparse result.

However, current sparse regression techniques face certain difficulty when the number of candidate functions p is large and especially when candidate functions contain trigonometric functions. To ensure a sparse and accurate solution, we propose a trial-and-error method in which we denote the maximum number of meaningful terms by k (which is small compared with p) and perform a search over all possible combinations of k terms in the domain of p terms.

We here aim to incorporate prior knowledge of simple systems that form the complex system. Denoting the total energy of an element in the system as E_i, the total energy of the whole system is the sum of all elements: $E = \sum_i E_i$. It is therefore reasonable to assume that the candidate functions that appear in constituents do appear in the combination. If h terms can be retained, the number of trials decreases to $\binom{p-h}{k-h}$.

Our challenge is now to solve (4) for a reduced $\boldsymbol{\Gamma}(\mathbf{X}, \dot{\mathbf{X}})$ (written as $\boldsymbol{\Gamma}_r(\mathbf{X}, \dot{\mathbf{X}})$) and to select the best match(es) by comparing the L^2-norm to a threshold:

$$\left\| \boldsymbol{\Gamma}_r(\mathbf{X}, \dot{\mathbf{X}})\boldsymbol{\xi} - \frac{d\mathbf{E}}{dt} \right\|^2 < threshold. \tag{5}$$

In the case of a passive system, the trivial solution $\boldsymbol{\xi} = \mathbf{0}$ should be avoided. Therefore, an additional condition $\|\boldsymbol{\xi}\|^2 > threshold$ should be applied.

B. Finding the Lagrangian from learned energy

Under certain conditions that generalized coordinates do not have an explicit time dependency and forces are derivable from a conservative potential, the total energy and Hamiltonian coincide [14]. Generally, for popular mechanical systems in the field of robotics, these conditions are satisfied if the effect of friction is neglected. We further discuss this issue in section II-D. Henceforth, the total energy is referred as the Hamiltonian.

In classical mechanics, a Hamiltonian function $\mathrm{H}(\mathbf{q}, \mathbf{p})$ is constructed from the Legendre transformation of a Lagrangian function $\mathrm{L}(\mathbf{q}, \dot{\mathbf{q}})$ as

$$\mathrm{H}(\mathbf{q}, \mathbf{p}) = \dot{\mathbf{q}}\mathbf{p} - \mathrm{L}(\mathbf{q}, \dot{\mathbf{q}}), \tag{6}$$

where canonical coordinates are denoted $\mathbf{q}$ and canonical momenta are denoted $\mathbf{p} = [p_1\,p_2\,\cdots\,p_n]^T = [\frac{\partial \mathrm{L}}{\partial \dot{q}_1}\,\frac{\partial \mathrm{L}}{\partial \dot{q}_2}\cdots\frac{\partial \mathrm{L}}{\partial \dot{q}_n}]^T$.

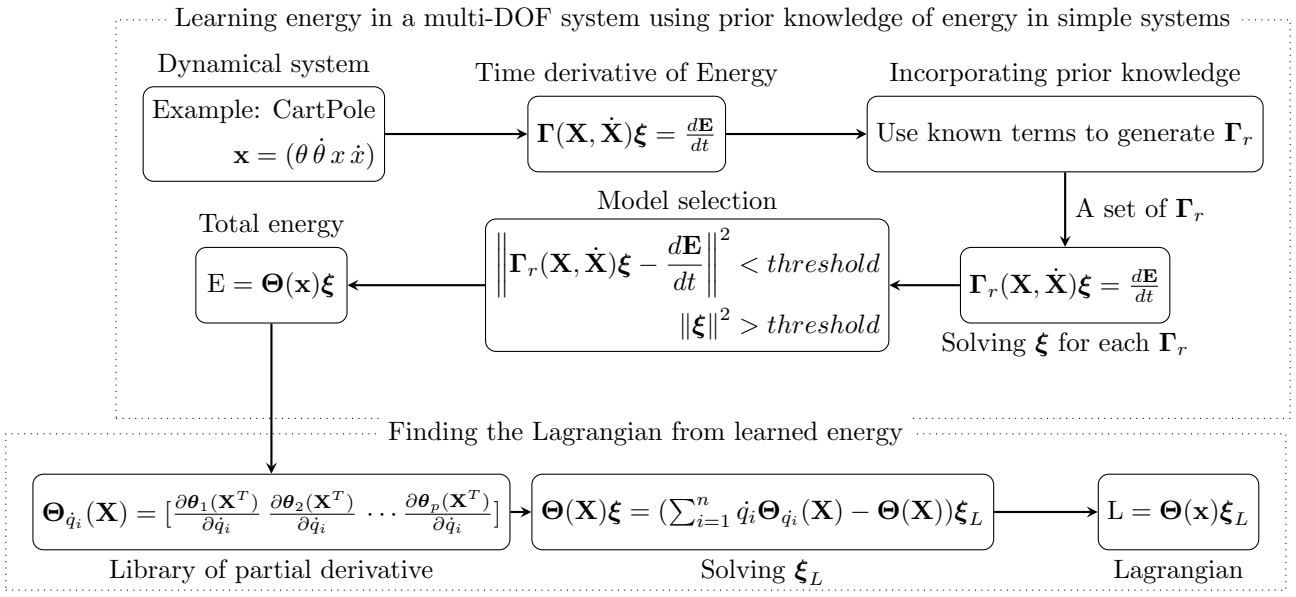

Fig. 1. Block diagram showing the learning of energy in a multi-DOF system using prior knowledge of energy in simple systems and finding the Lagrangian from the learned energy. Our main contributions are incorporating knowledge to generate a set of Γ_r in the third step and finding the Lagrangian.

The aforementioned process suggests that once a Lagrangian is known, the corresponding Hamiltonian can be constructed. We propose a method of performing the reverse process; i.e., extracting a Lagrangian from a known Hamiltonian.

Because both the Lagrangian and Hamiltonian are formed from kinetic energy and potential energy, it is possible to assume that the candidate functions used to build the Hamiltonian are sufficient to represent the corresponding Lagrangian. The library of nonlinear terms used for modeling the total energy $\mathbf{\Theta}(\mathbf{X})$ is therefore reused, and the Lagrangian is characterized as $\mathbf{\Theta}(\mathbf{X})\boldsymbol{\xi}_L$. The Legendre transformation in (6) is rewritten as

$$\mathbf{\Theta}(\mathbf{X})\boldsymbol{\xi} = (\sum_{i=1}^{n} \dot{q}_i \mathbf{\Theta}_{\dot{q}_i}(\mathbf{X}) - \mathbf{\Theta}(\mathbf{X}))\boldsymbol{\xi}_L, \tag{7}$$

where $\mathbf{\Theta}_{\dot{q}_i}(\mathbf{X}) = [\frac{\partial \boldsymbol{\theta}_1(\mathbf{X}^T)}{\partial \dot{q}_i}\ \frac{\partial \boldsymbol{\theta}_2(\mathbf{X}^T)}{\partial \dot{q}_i}\ \cdots\ \frac{\partial \boldsymbol{\theta}_p(\mathbf{X}^T)}{\partial \dot{q}_i}]$. Solving this linear equation yields $\boldsymbol{\xi}_L$, and the Lagrangian can thus be effectively constructed.

C. Scaling in a passive system

If no energy is supplied or withdrawn from a system, the total energy should stay constant. Thus, the solution to (4) gives $\boldsymbol{\xi}$ with which to construct $\mathbf{E}$ as in (2) such that $\frac{d\mathbf{E}}{dt} = \mathbf{0}$. It is clear that if $\mathbf{E}$ is modified by a constant multiplication factor k, the constraint $\frac{d\mathbf{E}}{dt} = \mathbf{0}$ still holds. Therefore, an additional step is required to discover the scaling factor and find the true formula of energy.

We suggest using additional data captured in a short time interval (even at only one time is sufficient in some cases) when actuation is available. In that case, we have access to non-zero $\frac{d\mathbf{E}}{dt}$, and the true vector of coefficients $\boldsymbol{\xi}_{true} = k\boldsymbol{\xi}$ should thus be a solution of (4). k is the only unknown value, and solving for k can therefore be done simply by linear regression:

$$\mathbf{\Gamma}(\mathbf{X}, \dot{\mathbf{X}})(k\boldsymbol{\xi}) = \frac{d\mathbf{E}}{dt}. \tag{8}$$

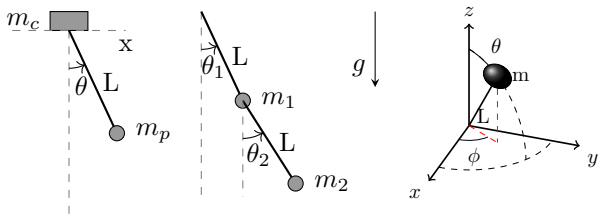

Fig. 2. Three dynamical systems. From left to right: the cart-pendulum system, double pendulum and spherical pendulum. In all systems, the length of the rod is $\mathrm{L} = 1.0\mathrm{m}$ and gravitational acceleration is $\mathrm{g} = 9.8\mathrm{m/s^2}$. Cart-pendulum system: $\mathrm{m_c} = 1.0\mathrm{kg}$, $\mathrm{m_p} = 0.1\mathrm{kg}$, and the actuation is a force acting on $\mathrm{m_c}$. Double pendulum: $\mathrm{m_1} = 1.0\mathrm{kg}$, $\mathrm{m_2} = 1.0\mathrm{kg}$, and the actuation is a moment acting on the first link. Spherical pendulum: $\mathrm{m} = 1.0\mathrm{kg}$, and the actuation is a moment on the xy-plane.

D. Dynamical systems and experiments

We employ three idealized multi-DOF nonlinear systems as objects for experiments. In all systems, data are sampled at 100 Hz and gravity is the only external force. Therefore, conditions that the Hamiltonian and total energy coincide are satisfied.

We test actuated and passive schemes on each system. In the actuated scheme, the system is actuated by the actuation described in the caption of Fig. 2, which is set to $1.0\mathrm{N}$ in the

TABLE I
HAMILTONIAN AND LAGRANGIAN EXTRACTED FROM SIMULATION DATA

Quantities	Physical systems		
	Spherical pendulum	***Double pendulum***	***Cart-Pendulum***
Hamiltonian	$\frac{1}{2}mL^2(\dot{\theta}^2+\dot{\phi}^2\sin^2\theta)$ $+mgL\cos\theta$	$\frac{1}{2}(m_1+m_2)L^2\dot{\theta_1}^2+\frac{1}{2}m_2L^2\dot{\theta_2}^2+m_2L^2\dot{\theta_1}\dot{\theta_2}\cos(\theta_1-\theta_2)$ $-(m_1+m_2)gL\cos\theta_1-m_2gL\cos\theta_2$	$\frac{1}{2}(m_c+m_p)\dot{x}^2+\frac{1}{2}L^2\dot{\theta}^2$ $+m_pL\dot{x}\dot{\theta}\cos\theta-m_pgL\cos\theta$
Lagrangian	$\frac{1}{2}mL^2(\dot{\theta}^2+\dot{\phi}^2\sin^2\theta)$ $+mgL\cos\theta$	$\frac{1}{2}(m_1+m_2)L^2\dot{\theta_1}^2+\frac{1}{2}m_2L^2\dot{\theta_2}^2+m_2L^2\dot{\theta_1}\dot{\theta_2}\cos(\theta_1-\theta_2)$ $+(m_1+m_2)gL\cos\theta_1+m_2gL\cos\theta_2$	$\frac{1}{2}(m_c+m_p)\dot{x}^2+\frac{1}{2}L^2\dot{\theta}^2$ $+m_pL\dot{x}\dot{\theta}\cos\theta+m_pgL\cos\theta$
Hamiltonian[a]	$0.500\dot{\phi}^2\sin^2\theta+0.500\dot{\theta}^2$ $-9.810\cos\theta$	$1.000\dot{\theta_1}^2+0.500\dot{\theta_2}^2+1.000\dot{\theta_1}\dot{\theta_2}\cos\theta_1\cos\theta_2$ $+1.000\dot{\theta_1}\dot{\theta_2}\sin\theta_1\sin\theta_2-19.620\cos\theta_1-9.810\cos\theta_2$	$0.550\dot{x}^2+0.050\dot{\theta}^2$ $+0.100\dot{\theta}\dot{x}\cos\theta-0.981\cos\theta$
Lagrangian[a]	$0.500\dot{\phi}^2\sin^2\theta+0.500\dot{\theta}^2$ $-9.810\cos\theta$	$1.000\dot{\theta_1}^2+0.500\dot{\theta_2}^2+1.000\dot{\theta_1}\dot{\theta_2}\cos\theta_1\cos\theta_2$ $+1.000\dot{\theta_1}\dot{\theta_2}\sin\theta_1\sin\theta_2+19.620\cos\theta_1+9.810\cos\theta_2$	$0.550\dot{x}^2+0.050\dot{\theta}^2$ $+0.100\dot{\theta}\dot{x}\cos\theta+0.981\cos\theta$
Hamiltonian[p]	x	$1.000\dot{\theta_1}^2+0.500\dot{\theta_2}^2+1.000\dot{\theta_1}\dot{\theta_2}\cos\theta_1\cos\theta_2$ $+1.000\dot{\theta_1}\dot{\theta_2}\sin\theta_1\sin\theta_2-19.620\cos\theta_1-9.810\cos\theta_2$	$0.550\dot{x}^2+0.050\dot{\theta}^2$ $+0.100\dot{\theta}\dot{x}\cos\theta-0.981\cos\theta$
Lagrangian[p]	x	$1.000\dot{\theta_1}^2+0.500\dot{\theta_2}^2+1.000\dot{\theta_1}\dot{\theta_2}\cos\theta_1\cos\theta_2$ $+1.000\dot{\theta_1}\dot{\theta_2}\sin\theta_1\sin\theta_2+19.620\cos\theta_1+9.810\cos\theta_2$	$0.550\dot{x}^2+0.050\dot{\theta}^2$ $+0.100\dot{\theta}\dot{x}\cos\theta+0.981\cos\theta$
Hamiltonian[an]	$0.500\dot{\phi}^2\sin^2\theta+0.500\dot{\theta}^2$ $+9.810\cos\theta$	x	$0.550\dot{x}^2+0.050\dot{\theta}^2$ $+0.100\dot{\theta}\dot{x}\cos\theta-0.981\cos\theta$
Lagrangian[an]	$0.500\dot{\phi}^2\sin^2\theta+0.500\dot{\theta}^2$ $-9.810\cos\theta$	x	$0.550\dot{x}^2+0.050\dot{\theta}^2$ $+0.100\dot{\theta}\dot{x}\cos\theta+0.981\cos\theta$

[a]Result for the actuated scheme,[p]Result for the passive scheme,[n]Result when data are corrupted by Gaussian noise$\mathcal{N}(\mu,\sigma)$ $(\mu=0,\sigma=1e-8)$
All numbers are rounded to three decimal places. Parameters of the systems are written in the caption of Fig. 2

case of a force or $1.0\mathrm{Nm}$ in the case of a moment, and data are collected for a period of 1 s. In the passive scheme, the actuation is set to zero and data are collected for a period of 3 s. The second trial for getting the multiplication factor of $\boldsymbol{\xi}$ is completed in 0.1 s.

The obtained analytical form of the Lagrangian is further processed by calculating the Euler–Lagrange equations using Lagrange's method in Sympy [18], to get the differential equations that reveal the underlying dynamics. We evaluate the results by taking the integral of these equations and comparing with the true data. Furthermore, we use the extracted model for swinging up the cart-pendulum system using a controller based on model predictive control.

We test our proposed method against SINDy and KRONIC. The tested solver in SINDy is Lasso, while in KRONIC, the vector of coefficients $\boldsymbol{\xi}$ is the eigenvector corresponding to the smallest eigenvalue that is calculated by singular value decomposition.

III. RESULTS

In this section, we demonstrate that Lagrangian-SINDy effectively finds the total energy in three test systems and accurately obtain the Lagrangian from the energy. Both forms and coefficients are accurately calculated, resulting in the discovery of physical laws that are close to the true underlying dynamics (Table I).

In addition, we reveal that our tight constraints on sparsity give the sparsest result among the methods adopted (Fig. 3). Our results have notably good accuracy in that our simulation using the identified equations of motion matches the simulation using the true equations of motion (Fig. 4).

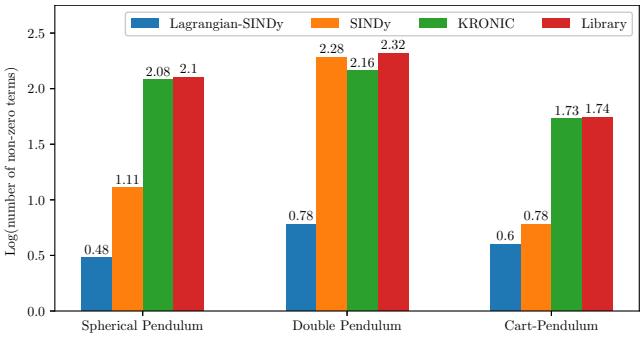

Fig. 3. Comparison of the resulting model complexity for three methods: SINDy, KRONIC and Lagrangian-SINDy. Data are also compared with the library as a reference. A lower value indicates a sparser representation. All results are obtained using the actuated scheme for Lagrangian-SINDy and SINDy. KRONIC is tested using the passive scheme as it searches for conserved quantities.

A. Spherical pendulum

The state of the spherical pendulum is described as $\mathbf{x}=[\theta\,\dot{\theta}\,\phi\,\dot{\phi}]^T$. To include all nonlinear terms that sufficiently describe the Hamiltonian and Lagrangian, a library of functions is created as all polynomial combinations of $[\cos\theta\ \sin\theta, \dot{\theta}\,\phi\,\dot{\phi}]$ up to fourth order. The initial condition for simulation is $\mathbf{x}_{init}=[\frac{\pi}{2}\,0\,0\,0.5]^T$.

In this experiment, no prior knowledge is used to boost the learning process because this system is the simplest pendulum-type system in three dimensions.

1) Actuated scheme: Additional information on how energy changes is provided to support the learning process. The resulting Hamiltonian and Lagrangian match true values. The

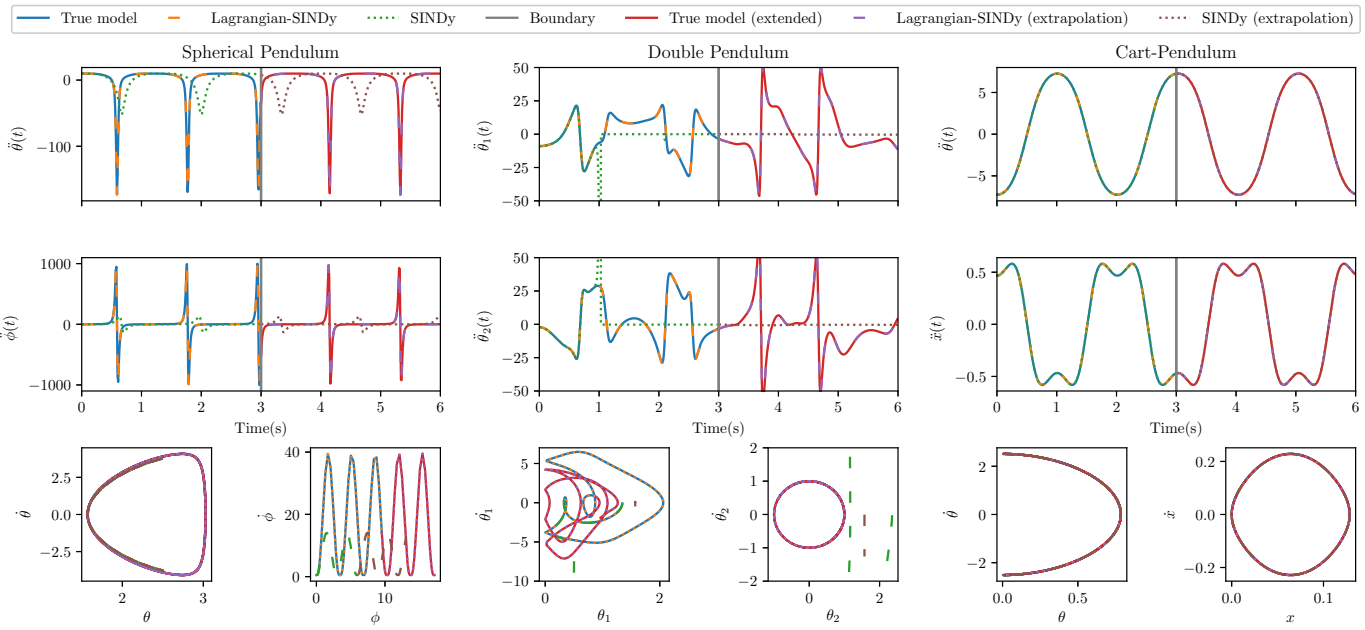

Fig. 4. Simulation results for various models: the true model, Lagrangian-SINDy discovered model and SINDy identified model. Data are simulated in the first 3 seconds (with no actuation), and extrapolation (exploring beyond the learning dataset) is then tested in the next 3 seconds and shown on the right side of the boundary line. Results are shown for three systems (i.e., the spherical pendulum, double pendulum and cart-pendulum system) in terms of acceleration (in the first and second rows) and the phase portrait (in the third row). The accuracy of our Lagrangian-SINDy over SINDy can be observed from the plots against the simulated ground truth.

same result is recovered when data are corrupted by Gaussian noise.

Using Lagrange's method and considering the actuation as u, equations of motion are obtained as

$$\begin{aligned} \ddot{\theta} &= 1.000\cos\theta\dot{\phi}^2 + 9.810\cos\theta, \\ \ddot{\phi} &= \frac{1.000(u - \dot{\phi}\dot{\theta}\sin 2\theta)}{\sin^2\theta}. \end{aligned} \tag{9}$$

Equations (9) suggest that a rational function is required to obtain the correct physical law. However, because rational functions are not included in the library, SINDy encounters difficulty because it tries to build equations of motion directly from the basis functions.

Both SINDy and Lagrangian-SINDy reveal periodic features in $\ddot{\theta}$ and $\ddot{\phi}$; however, our results are more accurate.

2) Passive scheme: It appears that no result can pass our model selection filter; therefore, the passive situation is concluded to be difficult for Lagrangian-SINDy.

B. Double pendulum

Denoting the state of the double pendulum by $\mathbf{x} = [\theta_1\ \dot{\theta}_1\ \theta_2\ \dot{\theta}_2]^T$, a library containing polynomial combinations of $[\cos\theta_1, \sin\theta_1, \dot{\theta}_1, \cos\theta_2, \sin\theta_2, \dot{\theta}_2]$ with degree less than or equal to four is built. Data are simulated for the initial condition $\mathbf{x}_{init} = [\frac{3\pi}{7}\ 0\ \frac{3\pi}{4}\ 0]^T$.

If we denote a pendulum's angle by θ, the mass by m and the length by L, the energy is describe as $E = \frac{1}{2}mL^2\dot{\theta}^2 - mgL\cos\theta$. As a result, four terms $\cos\theta_1, \dot{\theta}_1^2, \cos\theta_2, \dot{\theta}_2^2$ are forced to appear in $\mathbf{\Gamma}_r$. Two additional terms are selected from the remaining terms in the library.

The extracted quantities do not appear to be the same as the true physical expressions, yet match their trigonometric expansions. These results are in fact logical, as the exact expression of $\cos(\theta_1 - \theta_2)$ cannot be found because it does not exist in the library. Instead, a quantity that is approximately equal to the expansion is built from the existing basis functions.

The calculated equations of motion show that $\ddot{\theta}_1$ and $\ddot{\theta}_2$ are rational functions and their denominators depend on both θ_1 and θ_2. The original SINDy method, which is incapable of finding a rational function, still performs well in estimating both $\ddot{\theta}_1$ and $\ddot{\theta}_2$ within a horizon of approximately 1 second, and diverges later.

In this experiment, good results are obtained for both actuated and passive schemes. However, no result passes our model selection under the disturbance of a low level of Gaussian noise $\mathcal{N}(0, 10^{-8})$. We experimentally found that the maximum noise level that can be managed is $\mathcal{N}(0, 10^{-9})$.

C. Cart-pendulum system

Similar to the two previous examples, if the state is represented as $\mathbf{x} = [\theta\ \dot{\theta}\ x\ \dot{x}]^T$, we construct a library by combining polynomial features of $[\cos\theta, \sin\theta, \dot{\theta}, x, \dot{x}]$ up to the degree of three. Data are generated by computer simulation with the initial condition $\mathbf{x}_{init} = [\frac{\pi}{4}\ 0\ 0\ 0]^T$.

The two terms $\dot{\theta}^2$ and $\cos\theta$ are forced to be in $\mathbf{\Gamma}_r$ as they come from knowledge of a simple pendulum. Two more

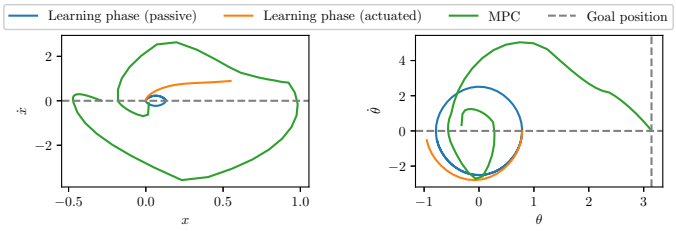

Fig. 5. Training trajectory (in two schemes) and model predictive controlled trajectory of the cart-pendulum system in the cart's phase portrait (left) and the pendulum's phase portrait (right).

terms are selected from the remaining terms in the library.

The equations of motion are calculated using Lagrange's method (considering the actuation as u and neglecting any term that has a coefficient of 10^{-17} or smaller):

$$\begin{aligned}\ddot{\theta} &= \frac{1.000(1.000u\cos\theta + 10.791\sin\theta + 0.050\sin(2\theta)\dot{\theta}^2}{0.100\cos^2\theta - 1.100},\\ \ddot{x} &= \frac{(1.000u + 0.100\sin\theta\dot{\theta}^2 + 0.490\sin(2\theta)}{0.100\cos^2\theta - 1.100}.\end{aligned} \tag{10}$$

Both SINDy and Lagrangian-SINDy perform well in tracking the physical evolution of this system. However, as the library does not contain rational functions, the equations generated by SINDy cannot be displayed in their exact form. In this case, the SINDy model is not interpretable despite having high accuracy.

We further use (10) for model predictive control [19]. From a random initial condition, the controller successfully swings the pole upward by pushing the cart. The force is set to have one of three values: 10, 0 or -10N. The resulting motion of the controlled system (shown in Fig. 5) is similar to the results of [6].

IV. Discussion and Conclusion

With Lagrangian-SINDy, we demonstrate the possibility of finding dynamics indirectly via energy-related physical quantities. This method does not seek expressions of time derivatives of the state and instead searches for a single Lagrangian that shelters the hidden dynamics. Equations of motion are later distilled by applying general knowledge in classical mechanics.

One important factor is the construction of the library containing nonlinear functions. A large library is more likely to contain sufficient basis functions with which to reconstruct physical quantities; however, the number of possible combinations increases tremendously if the library is exceedingly large. As a result, the computational load rises and the learning process slows. If the library is small and does not contain the exact necessary terms, Lagrangian-SINDy may find an approximation, in a manner similar to what was reported in [4]; however, this does not guarantee the precision of the eventual equations of motions.

For the three idealized systems used in the experiment, Lagrangian-SINDy finds the Hamiltonian and the corresponding Lagrangian by combining non-rational functions, while rational functions are required to discover the true equations of motion. Therefore, this simplification is possibly considered an advantage over the original SINDy method. If rational functions are included in the library, the learning pace is potentially lowered as previously mentioned.

The sparsity constraint (i.e., k, the number of terms to be selected from the library to build $\mathbf{\Gamma}_r$) is substantial. A large value of k may lead to a huge number of combinations, exponentially increasing the learning time. A small value of k ensures sparse results and sufficiently low computational cost; however, a problem of under-fitting may be encountered.

As [4] pointed out, knowledge from simple systems can be used to bootstrap the learning process. However, the reason for using knowledge from simple systems is unclear in the cited work. In Lagrangian-SINDy, because the total energy of a complex system is the sum of all elements' energies, it is straightforward to linearly combine the terms that build up energies of the simple systems to obtain the total energy. Reusing these terms indicates that results should be in the form of energy and reduces the number of combinations to be tested.

Our results indicate that additional information on how total energy varies in time is crucial. In the case of a passive system, energy is conserved and Lagrangian-SINDy is similar to KRONIC in that it searches for conserved quantities and selects the one most likely to be the total energy. In the case of an actuated system, we search for a quantity that varies in time equally to the change of a given quantity, and the criterion is thus strict and more explicit. Under ideal conditions (i.e., when noise is eliminated), results for the spherical pendulum can be found in the actuated scheme, while this difficulty cannot be overcome in the passive scheme.

Noise, which almost always exists in a real system, has a notable effect on the performance of Lagrangian-SINDy. Our method is sensitive to noise, as we reported that the maximum Gaussian noise level that it can handle for the spherical pendulum and cart-pendulum system is $\mathcal{N}(0, 10^{-8})$, which changes the total energy by a proportion of less than one millionth. The main reason for this disadvantage is that noise is amplified during the formation of $\mathbf{\Gamma}(\mathbf{X}, \dot{\mathbf{X}})$ owing to the chain rule. Improving the noise robustness of Lagrangian-SINDy is essential for further applications to real systems, and we leave this task as future work.

Another possible extension is implementing Lagrangian-SINDy on non-conservative systems. This extension is currently an arduous task because damping results in energy loss. However, we believe that the extension is not impossible. Eigenvectors corresponding to small eigenvalues may include the correct solution, because they may relate to a lightly damped system [12].

Reduced or approximate dynamical models are widely used in practice because of the complexity of real dynamical systems; however, an accurate model of full dynamics can

provide better precision in prediction, estimation and control. With Lagrangian-SINDy, we hope to create machines that can autonomously find accurate nonlinear dynamics and potentially improve tool manipulation and part interchangeability for robots (similar to that achieved in [20] [21]). Analytical and non-analytical approaches would support each other to understand dynamical models with diverse perspectives.

REFERENCES

[1] M. I. Jordan and T. M. Mitchell, "Machine learning: Trends, perspectives, and prospects," *Science*, vol. 349, no. 6245, pp. 255–260, 2015. [Online]. Available: https://science.sciencemag.org/content/349/6245/255

[2] V. Marx, "Biology: The big challenges of big data," *Nature*, vol. 498, pp. 255–60, 06 2013.

[3] M. T. Ribeiro, S. Singh, and C. Guestrin, ""why should i trust you?": Explaining the predictions of any classifier," in *Proceedings of the 22nd ACM SIGKDD International Conference on Knowledge Discovery and Data Mining*, ser. KDD '16. New York, NY, USA: Association for Computing Machinery, 2016, p. 1135–1144. [Online]. Available: https://doi.org/10.1145/2939672.2939778

[4] M. Schmidt and H. Lipson, "Distilling free-form natural laws from experimental data," *Science*, vol. 324, no. 5923, pp. 81–85, 2009. [Online]. Available: https://science.sciencemag.org/content/324/5923/81

[5] S. S. Sahoo, C. H. Lampert, and G. Martius, "Learning equations for extrapolation and control," *CoRR*, vol. abs/1806.07259, 2018. [Online]. Available: http://arxiv.org/abs/1806.07259

[6] S. Sahoo, C. Lampert, and G. Martius, "Learning equations for extrapolation and control," in *Proceedings of the 35th International Conference on Machine Learning*, ser. Proceedings of Machine Learning Research, J. Dy and A. Krause, Eds., vol. 80. Stockholmsmässan, Stockholm Sweden: PMLR, 10–15 Jul 2018, pp. 4442–4450. [Online]. Available: http://proceedings.mlr.press/v80/sahoo18a.html

[7] S. L. Brunton, J. L. Proctor, and J. N. Kutz, "Discovering governing equations from data by sparse identification of nonlinear dynamical systems," *Proceedings of the National Academy of Sciences*, vol. 113, no. 15, pp. 3932–3937, 2016. [Online]. Available: https://www.pnas.org/content/113/15/3932

[8] S. H. Rudy, S. L. Brunton, J. L. Proctor, and J. N. Kutz, "Data-driven discovery of partial differential equations," *Science Advances*, vol. 3, no. 4, 2017. [Online]. Available: https://advances.sciencemag.org/content/3/4/e1602614

[9] S. L. Brunton, J. L. Proctor, and J. N. Kutz, "Sparse identification of nonlinear dynamics with control (sindyc)," *IFAC-PapersOnLine*, vol. 49, no. 18, pp. 710 – 715, 2016, 10th IFAC Symposium on Nonlinear Control Systems NOLCOS 2016. [Online]. Available: http://www.sciencedirect.com/science/article/pii/S2405896316318298

[10] N. M. Mangan, S. L. Brunton, J. L. Proctor, and J. N. Kutz, "Inferring biological networks by sparse identification of nonlinear dynamics," *IEEE Transactions on Molecular, Biological and Multi-Scale Communications*, vol. 2, no. 1, pp. 52–63, June 2016.

[11] M. Quade, M. Abel, J. Nathan Kutz, and S. L. Brunton, "Sparse identification of nonlinear dynamics for rapid model recovery," *Chaos: An Interdisciplinary Journal of Nonlinear Science*, vol. 28, no. 6, p. 063116, 2018. [Online]. Available: https://doi.org/10.1063/1.5027470

[12] E. Kaiser, J. N. Kutz, and S. L. Brunton, "Data-driven discovery of Koopman eigenfunctions for control," *arXiv e-prints*, p. arXiv:1707.01146, Jul 2017.

[13] ——, "Discovering conservation laws from data for control," in *2018 IEEE Conference on Decision and Control (CDC)*, Dec 2018, pp. 6415–6421.

[14] H. Goldstein, C. Poole, and J. Safko, *Classical Mechanics*. Addison Wesley, 2002. [Online]. Available: https://books.google.co.jp/books?id=tJCuQgAACAAJ

[15] G. H. Golub and C. Reinsch, "Singular value decomposition and least squares solutions," *Numerische Mathematik*, vol. 14, no. 5, pp. 403–420, Apr 1970. [Online]. Available: https://doi.org/10.1007/BF02163027

[16] A. N. Tikhonov and V. Y. Arsenin, *Solutions of ill-posed problems*. Washington, D.C.: John Wiley & Sons, New York: V. H. Winston & Sons, 1977, translated from the Russian, Preface by translation editor Fritz John, Scripta Series in Mathematics.

[17] R. Tibshirani, "Regression shrinkage and selection via the lasso," *JOURNAL OF THE ROYAL STATISTICAL SOCIETY, SERIES B*, vol. 58, pp. 267–288, 1994.

[18] A. Meurer *et al.*, "Sympy: symbolic computing in python," *PeerJ Computer Science*, vol. 3, p. e103, Jan. 2017. [Online]. Available: https://doi.org/10.7717/peerj-cs.103

[19] B. Amos, I. D. J. Rodriguez, J. Sacks, B. Boots, and J. Z. Kolter, "Differentiable mpc for end-to-end planning and control," in *Proceedings of the 32nd International Conference on Neural Information Processing Systems*, ser. NIPS'18. Red Hook, NY, USA: Curran Associates Inc., 2018, p. 8299–8310.

[20] M. Hayashibe and S. Shimoda, "Synergetic learning control paradigm for redundant robot to enhance error-energy index," *IEEE Transactions on Cognitive and Developmental Systems*, vol. 10, no. 3, pp. 573–584, Sep. 2018.

[21] M. Hayashibe and S. Shimoda, "Synergetic motor control paradigm for optimizing energy efficiency of multijoint reaching via tacit learning," *Frontiers in Computational Neuroscience*, vol. 8, p. 21, 2014. [Online]. Available: https://www.frontiersin.org/article/10.3389/fncom.2014.00021